Cite this: *Analyst*, 2011, **136**, 2802

www.rsc.org/analyst

PAPER

A novel baseline-correction method for standard addition based derivative spectra and its application to quantitative analysis of benzo(*a*)pyrene in vegetable oil samples

Na Li, Xiu-Ying Li, Zhe-Xiang Zou, Li-Rong Lin and Yao-Qun Li*

Received 25th September 2010, Accepted 2nd May 2011
DOI: 10.1039/c0an00751j

In the present work, a baseline-correction method based on peak-to-derivative baseline measurement was proposed for the elimination of complex matrix interference that was mainly caused by unknown components and/or background in the analysis of derivative spectra. This novel method was applicable particularly when the matrix interfering components showed a broad spectral band, which was common in practical analysis. The derivative baseline was established by connecting two crossing points of the spectral curves obtained with a standard addition method (SAM). The applicability and reliability of the proposed method was demonstrated through both theoretical simulation and practical application. Firstly, Gaussian bands were used to simulate 'interfering' and 'analyte' bands to investigate the effect of different parameters of interfering band on the derivative baseline. This simulation analysis verified that the accuracy of the proposed method was remarkably better than other conventional methods such as peak-to-zero, tangent, and peak-to-peak measurements. Then the above proposed baseline-correction method was applied to the determination of benzo(*a*)pyrene (BaP) in vegetable oil samples by second-derivative synchronous fluorescence spectroscopy. The satisfactory results were obtained by using this new method to analyze a certified reference material (coconut oil, BCR®-458) with a relative error of −3.2% from the certified BaP concentration. Potentially, the proposed method can be applied to various types of derivative spectra in different fields such as UV-visible absorption spectroscopy, fluorescence spectroscopy and infrared spectroscopy.

1. Instruction

Derivative spectroscopy uses first- or higher-derivatives of spectral intensity with respect to wavelength for qualitative and quantitative analysis. The concept of derivative spectral data was first introduced in the 1950s.[1–4] The derivative technique has been proven very useful in improving the selectivity and sensitivity of a spectral analysis method. It has been applied widely in ultraviolet/visible absorption spectrophotometry[5–8] for the analysis of pharmaceutical, biological, food and environmental samples. This approach has also been applied to infrared spectroscopy,[9–12] and atomic flame emission and absorption spectroscopy.[13–15] The application of derivative techniques to luminescence spectroscopy was first proposed in 1974 by Green and O'Haver.[16] The combination of synchronous fluorescence spectroscopy and a derivative technique provided a better sensitivity than the conventional emission spectroscopy.[17,18] The combination of Constant-Energy Synchronous Luminescence (CESL) Spectroscopy with the derivative technique proposed by Li *et al.*[19] demonstrated an improvement to the selectivity and sensitivity of CESL.

The derivative technique usually improves the resolution of spectral bands, reduces the influence of background or matrix, and provides better-defined fingerprints than classical spectral approaches, since it enhances the detectability of minor spectral features such as weak shoulder peaks. Application of the derivative technique to spectroscopy offers a powerful tool for the quantitative analysis of multi-component mixtures by extracting qualitative and quantitative information from overlapping spectral bands of the analyte and interference.[20–22]

For quantitative spectral analysis, it was important to choose an appropriate method for the measurement of peak height. The ideal method for precise quantification of analytes should provide a value directly proportional to the target analyte concentration with zero intercept without interference. The most commonly employed measurement methods included peak-to-zero baseline measurement,[22–26] peak-to-peak measurement[27–31] and tangent methods.[32,33] However, a critical aspect in these measurements is the occurrence of background signals, causing error in the quantifications. Since it is a tough problem, massive efforts have been made to correct the baseline or to remove background.[34] Shao *et al.* developed some novel algorithms using

Department of Chemistry and Key Laboratory of Analytical Sciences, College of Chemistry and Chemical Engineering, Xiamen University, 361005, China. E-mail: yqlig@xmu.edu.cn

wavelet transform in denoising, baseline correction and detection of component number in overlapping chromatograms.[35–37] Liang and co-workers[38] proposed a method for baseline correction in spectroscopy data *via* adaptive iteratively reweighted penalized least squares. Zero-crossing measurement was also a common method for the simultaneous determination of binary mixtures with spectral overlapping,[39–41] where zero-crossing wavelength was selected by the individual derivative spectrum of each component. However, the zero-crossing method was difficult to be used in real samples showing matrix effects and/or unknown interferences.

In this work, we proposed a novel baseline-correction method referred to as peak-to-derivative baseline measurement for derivative spectral analysis. As is well known, the standard addition method (SAM) was one of the effective approaches[42–46] in reducing matrix effects. The derivative SAM spectra provided the information of overlapping bands of the analyte and the interference, and made it easy to identify two crossing points in the derivative spectra. Connecting these two points with a straight line formed the 'derivative baseline'. Deduction of the derivative baseline from the corresponding spectra reduced the error caused by the overlap of the analyte spectral band with unknown interfering bands. In order to demonstrate the feasibility of the proposed method, simulation analysis *via* computer-generated overlapping Gaussian band pairs was performed, where some conditions for the proposed method were discussed in detail, such as peak height, half-width of peaks, resolution of peaks, and the shape of the interference spectra. Then the proposed method was applied to the determination of a strong carcinogenic polycyclic aromatic hydrocarbon compound, benzo(*a*)pyrene, in oil samples by second-derivative constant-energy synchronous fluorescence spectroscopy (DCESFS). A certified reference material (coconut oil) BCR®-458 was used to examine the applicability and reliability of the proposed method.

2. Theoretical analysis

The theoretical analysis used here was based on computer-generated overlapping Gaussian band pairs: one was the 'analyte' band and the other the 'interfering' band. The analyte was measured in the presence of interference. A group of proportionally increased Gaussian bands were used to simulate the analyte band and the SAM bands with the increase of added analyte standard, assuming the amount of the simulated analyte was 1 (arbitrary unit) and the SAM bands with the increase of analyte from 1 to 3 (arbitrary unit). For the simulation analysis, several assumptions were made: (1) spectral bands were all a simple Gaussian shape, (2) the analyte band was overlapped with a single interfering band, (3) the total spectrum measured was the linear sum of the analyte and the interfering bands, and (4) derivatives were generated using only the information contained in the normal (zero-derivative) spectrum as ordinarily measured.

A Gaussian curve was generated by a Gaussian function of the form:

$$I(x) = ae^{-\frac{(x-b)^2}{2c^2}} \quad (1)$$

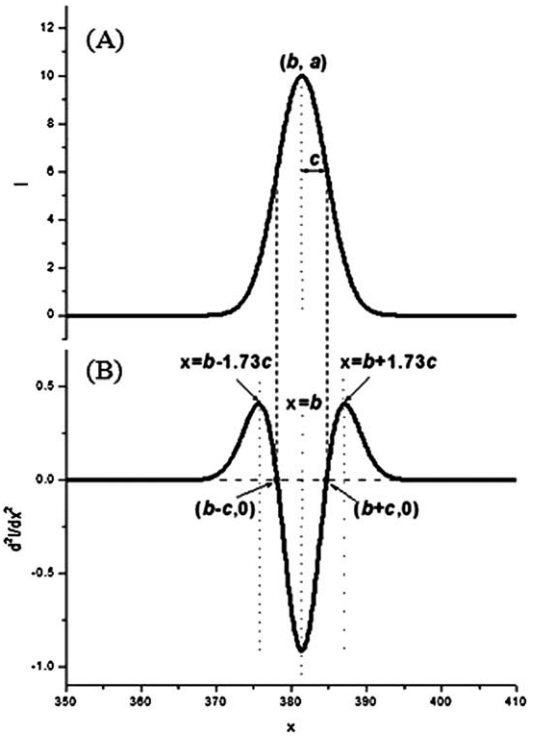

Fig. 1 Example of a Gaussian band (A) and its second-derivative curve (B).

where a is the height of the curve's peak, b is the position of the center of the peak, and c was the band half-width (more precisely, the standard deviation). The parameters of the Gaussian band and its second-derivative curve were shown in Fig. 1.

The band pair of overlapping bands was constructed by the sum of two Gaussian curves:

$$S(x) = a_1 e^{-\frac{(x-b_1)^2}{2{c_1}^2}} + a_2 e^{-\frac{(x-b_2)^2}{2{c_2}^2}} \quad (2)$$

The ratios of the interfering band parameters to the analyte band parameters were used to describe the band pair parameters.[47] Herein subscript 1 represents interfering band and subscript 2 represents analyte band. I = ratio of interfering band height to analyte band height = a_1/a_2. W = ratio of interfering band half-width to analyte half-width = c_1/c_2. S = ratio of band separation to half-width of analyte band = $(b_2 - b_1)/c_2$. The band pair shown in the insets of Fig. 2(B) would then be $I = 1$, $S = 1.5$ and $W = 2$.

2.1 Definition of derivative baseline

As shown in Fig. 2(A), the second-derivative curves of the target analyte band intersected with one another at two crossing points p_1 and p_2. The derivative line was constructed by connecting these two points (p_1 and p_2) by a straight line. When a pure analyte was measured, points p_1 and p_2 were in the zero baseline with the theoretical ordinate intensity at zero, *i.e.* $(b_2 - c_2, 0)$ and $(b_2 + c_2, 0)$, respectively, and thus the derivative baseline would be coincident with the zero baseline.

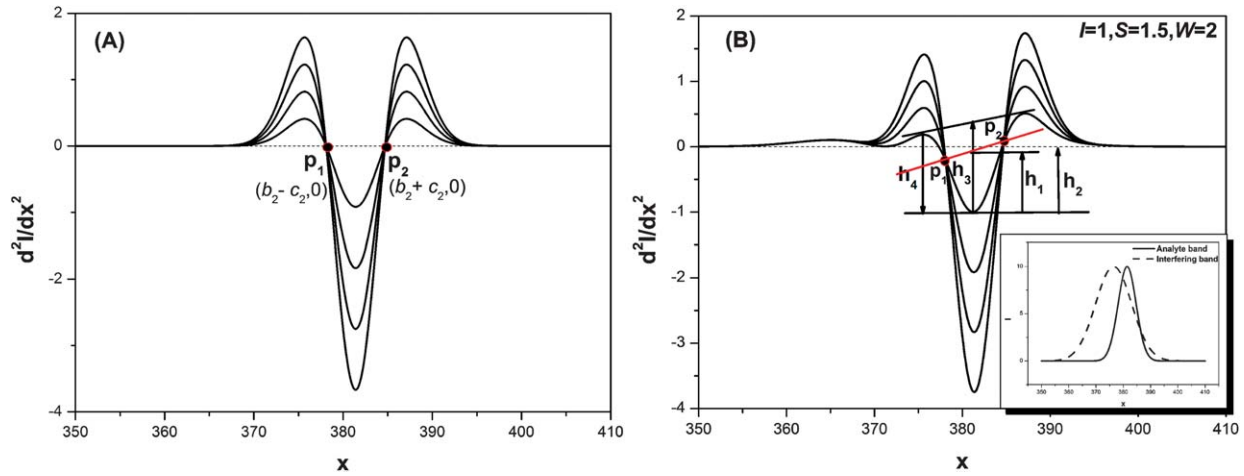

Fig. 2 Second-derivative curves of simulated analyte bands (assumed amount of analyte was 1, 2, 3 and 4 arbitrary units, respectively) without (A) and with interfering band (B). Dashed line: zero baseline; red line: derivative baseline. Definition of the measures: (h_1) peak-to-derivative baseline measurement; (h_2) peak-to-zero baseline measurement; (h_3) tangent measurement; (h_4) peak-to-peak measurement.

Fig. 2(B) shows the second-derivative curves of the sum of the interfering band and analyte bands and the standard addition sum curves. When the analyte band was measured in the presence of interference, the vertical coordinates of points p_1 and p_2 were superimposed with the interference curves, then the derivative baseline (red line) deviated from the zero baseline (black dashed line). It also means that p_1 and p_2 must be the points on the derivative curve of the interfering band. Although the second-derivative curve of unknown interference between points p_1 and p_2 cannot be determined in the real derivative spectrum detection, the derivative baseline is still closest to the interference curve. Therefore, the intensity value of the peak between points p_1 and p_2 deducted from the derivative baseline value (peak-to-derivative height) was used as the quantitative value.

In this simulation, the measures were constructed to represent the types of measurements which would be used in actual experimental studies. The techniques most commonly employed in the derivative sum curves included a peak-to-zero baseline measurement (h_2), a tangential approximation (h_3), and a peak-to-trough measurement (h_4). These measurement methods and the proposed peak-to-derivative baseline measurement (h_1) to correct for overlap with the interfering band were illustrated in Fig. 2(B). All these methods were used to obtain the concentration of the analyte by plotting the SAM calibration curves. The calibration curve was extrapolated to intersect with the concentration axis. The distance between the point of intersection and the point corresponding to the zero addition analyte concentration represented the measured analyte concentration in a sample. The relative errors, here defined as the relative percent difference between measured and 'actual' amount of analyte were determined for evaluating the accuracy of different measurement method.

2.2 Theoretical feasibility

In the analytical practice, the interfering band parameters might change from sample to sample or from measurement to measurement. For example, the interfering band might correspond to a single component whose concentration was only known approximately. In such a case the position of the center of peak b and half-width c were constant, but the height a could vary. In other systems, the interfering band could correspond to a mixture whose exact composition was unknown and varied from sample to sample. In these cases the relative half-width as well as the band separation could vary significantly. It was important to know how the derivative baseline was affected by changes in the parameters of the interfering band and whether the proposed methods reduced the error caused by the different interfering band or not, assuming that the parameters of the analyte band were constant.

During the investigation of different parameters, we observed that the relative errors were within $\pm 10.0\%$ when the S, and W values meet certain conditions, even though the interfering band intensity was up to 10 times the analyte band intensity (as shown in Table 1). Therefore, we investigated the effect of S, and W values on relative errors when $I \leq 10$.

Since the proposed derivative baseline is a straight line between two points, the smaller relative error was obtained when the derivative curve of the interference between these two points close to a straight line and the shape of the interference band is close to that of the baseline. The proposed method was suitable for the following situations:

(1) When the half-width of the interfering band is over four times than that of the analyte band ($W \geq 4$), the second-derivative curves of the interfering bands are smooth and the inflexion of the curve is inconspicuous. Thus, the derivative baseline will coincide with the second-derivative curves of the interfering bands, which makes the quantification more accurate. An example is illustrated in Fig. 3 for the case of $I = 10$, $S = 0$, $W = 4$, where the relative error was +4.9%.

(2) There are three extreme points whose curvature changed significantly on the second-derivative curves of the interfering bands at $x = b_1 - 1.7c_1$, $x = b_1$ and $x = b_1 + 1.7c_1$. Therefore, whether there were extreme points between the two crossing points p_1 and p_2 or not will determine whether the derivative baseline coincides with the second-derivative curves of the

Table 1 Relative errors (%) of measured analyte by proposed method for different parameters

	Relative error (%)						
I	$S = 1.5$, $W = 2$	$S = 1.5$, $W = 2.5$	$S = 2$, $W = 2.5$	$S = 2.5$, $W = 2.5$	$S = 1$, $W = 3$	$S = 3$, $W = 3.5$	$S = 0$, $W = 4$
0.5	+0.3	0	0	0	0	0	0
1	−0.5	+0.1	−0.1	−0.1	0	0	0
2	−0.5	+0.5	−0.5	−0.9	−0.1	−0.1	+1.2
5	−1.1	+4.0	−0.4	−4.9	+4.2	−0.1	+3.2
10	−1.2	+4.9	−1.2	−9.7	+8.7	−4.4	+4.9

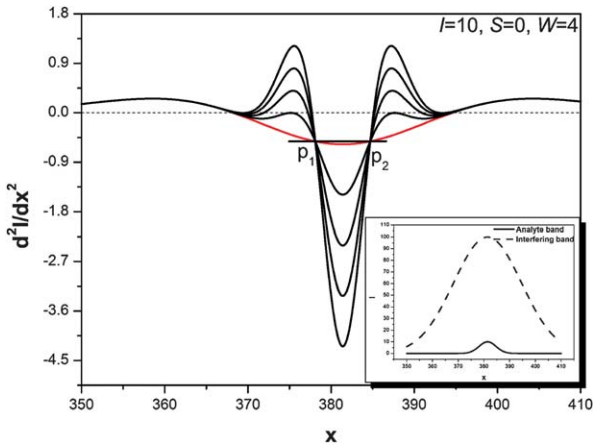

Fig. 3 Example of broader interfering band for the case $I = 10$, $S = 0$, $W = 4$.

interfering bands or not, thus determining the magnitude of the relative errors. Since the second-derivative curves were symmetrical, we took the interfering curve in the left side of analyte curve ($b_2 \geq b_1$) as an example for discussion.

When extreme points $x = b_1$, $x = b_1 + 1.7c_1$ of the second-derivative curve of the interfering band were not between the two crossing points p_1 and p_2, the derivative baseline would be in better accordance with the second-derivative curves of the interfering bands between points p_1 and p_2, and thus the measurement result is accurate and the relative error is small. As shown in Fig. 4(A) for the case $I = 1$, $S = 1.5$, $W = 2$, the relative error was −0.51%. Conversely, when the extreme points fell into the two crossing points p_1 and p_2, the shape of the baseline deviates from that of the interference band significantly, resulting in the large relative error. As shown in Fig. 4(B) for the case $I = 1$, $S = 2$, $W = 1.5$, the relative error was −10.9%.

Based on the above analysis, the inequalities were made as:

$$\begin{cases} b_1 \leq b_2 - c_2 & (3) \\ b_2 + c_2 \leq b_1 + 1.7c_1 & (4) \end{cases} \Longrightarrow \quad 1 \leq S \leq 1.7W - 1 \qquad (5)$$

Formula (5) can be expressed as $W \geq (S + 1)/1.7$ in the condition of $S \geq 1$, thus, when $S = 1$, the $W \geq 1.2$ can be deduced from these conditions. Therefore, the conditions fitted for formula (5) can be expressed as: (1) the distance between the center positions of the interfering bands and the analyte bands should not be less than the half-width peak of the analyte bands; and (2) the half-width peak of the interfering bands should not less than 1.2 times that of the analyte bands.

When S and W satisfy the above conditions, the measured amount of analyte obtained by the proposed measurement method was in a good agreement with the actual amount. An example is illustrated in Fig. 5 for the case $I = 1$, 2, 5 and 10, $S = 1.5$, and $W = 2.5$. In this figure, because the position and the half-width peak of the interfering band is settled, due to the effect of the different height of the interfering band, the derivative baseline deviates from zero baseline more obviously along with the stronger interfering band. The greater the peak intensity of the interfering band, the greater the degree of error. Nevertheless,

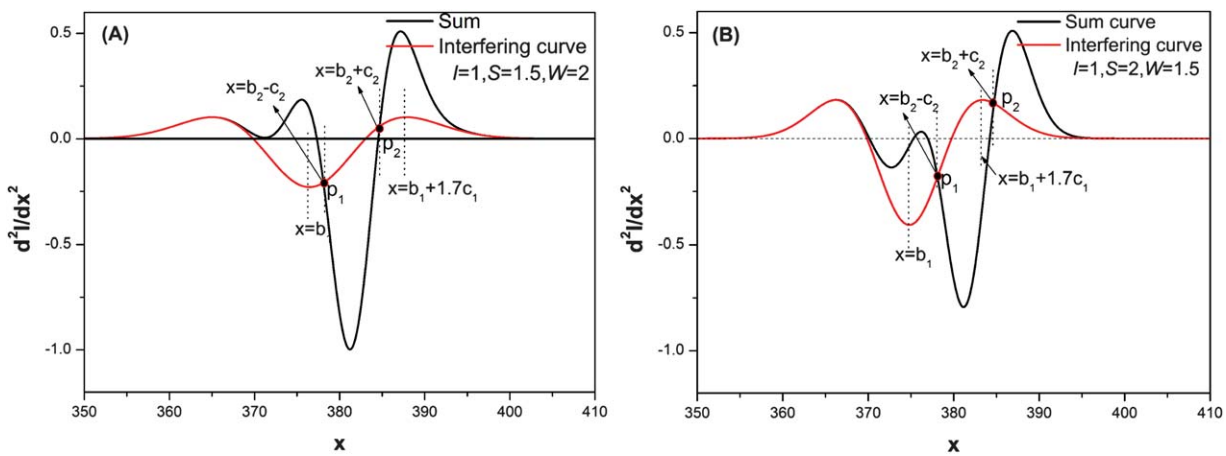

Fig. 4 Second-derivative curves of interfering and sum bands without (A) and with (B) extreme points between the two crossing points p_1 and p_2.

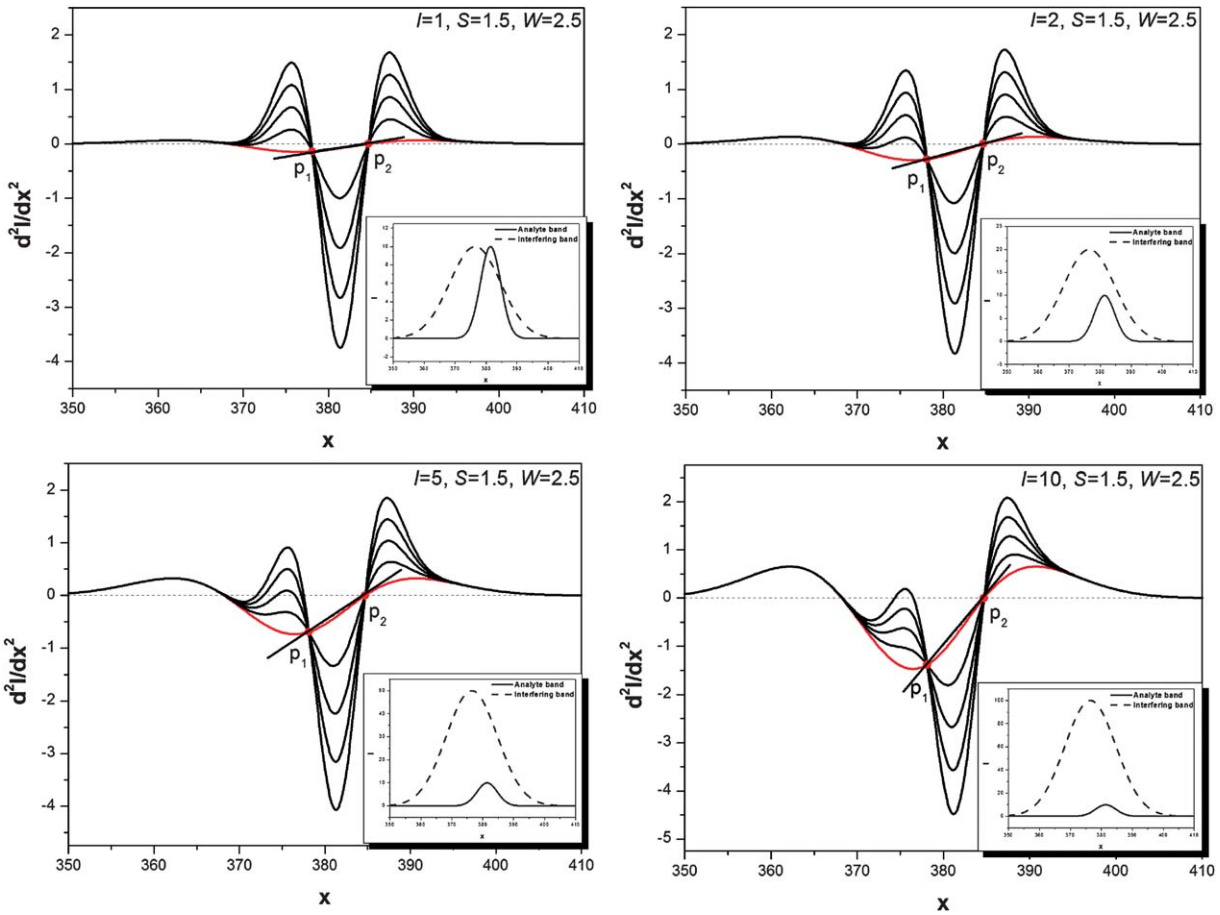

Fig. 5 Second-derivative sum curves with $I = 1$, 2, 5 and 10, for the case $S = 1.5$, $W = 2.5$. The red curve is the second-derivative curve of the interfering band; the black line is the derivative baseline; the dashed line is zero baseline. Inset: interfering band (black dashed curve) and analyte band (black solid curve) corresponding to each figure.

the relative error obtained by the proposed method was +4.9% at $I = 10$, even though the presence of the analyte peak was almost indistinguishable in the normal sum curve under these conditions. Thus, for $I \leq 10$, the proposed method still worked fine.

The proposed method was compared with traditional methods which were peak-to-zero baseline (h_2), tangent (h_3) and peak-to-trough (h_4) methods. The results are shown in Table 2, suggesting that the measured amount of analyte obtained by the proposed measurement method (h_1) was in a good agreement with the actual amount. Obviously, among these four methods, the proposed method was the best and the relative errors were significantly smaller than those obtained by the other three methods.

From these theoretical simulations, it can be concluded that the peak-to-derivative baseline method can get more accurate quantification results in the derivative spectra than traditional measurement methods.

3. Experimental

3.1 Instrumentation

Samples were saponificated using a domestic microwave oven (Galanz, G7020 II YSL-V1). The microwave-assisted saponification (MAS) process was carried out at 160 W for 10 min. A

Table 2 The relative errors of different S, and W values obtained by different measurement methods, for the case $I = 1$

	Relative error (%)			
Parameter	Peak-to-derivative baseline (h_1)	Peak-to-zero baseline (h_2)	Tangent (h_3)	Peak-to-trough (h_4)
$S = 1$, $W = 1$	−7.6	+30.8	+36.4	+32.0
$S = 1$, $W = 1.5$	−3.6	+17.8	+11.0	+20.4
$S = 1$, $W = 2$	−3.5	+16.9	+6.6	+17.8
$S = 1.5$, $W = 2.5$	−0.1	+8.7	+0.5	+9.3
$S = 1.5$, $W = 2$	−0.5	+8.8	+1.1	+13.7
$S = 2$, $W = 1.5$	−10.9	−13.5	−20.4	−37.7
$S = 1$, $W = 4$	−0.2	+5.7	+2.0	+2.2

glass of 500 mL of water was placed in the microwave oven for homogeneous heating.

All spectrofluorometric measurements were performed in a laboratory-constructed, computer-controlled spectrofluorometer. The spectrofluorometer was equipped with a 350-W xenon lamp (OSRAM GmbH, Steinerne Furt 6286167 Augsburg, Germany). The slit bandpass values of the excitation and emission monochromators were both set at 5 nm. The excitation and emission grating monochromators were controlled by a personal computer through a software package written in Turbo C 2.0. Experimental data were collected by the computer through the software package. In addition to conventional fluorescence spectra, the apparatus provided all types of synchronous spectra, including constant-wavelength, constant-energy, and variable-angle synchronous spectra. An electronic differentiator was connected to the spectrofluorometer for directly recording first- or second-derivative spectra. A 1 × 1 cm quartz cuvette was used for measurements throughout the study. This instrument has been used successfully in previous work.[19,48–50]

3.2 Materials and reagents

All of these vegetable oil samples were purchased from the supermarkets in Xiamen city, China.

A certified reference material (coconut oil, BCR®-458) was purchased from EC-JRC-IRMM, Belgium. The certified value of benzo(*a*)pyrene in the reference material was 0.93 μg kg^{-1}. Benzo (*a*)pyrene standard stock solution containing 100 μg mL^{-1} (97%, Sigma-Aldrich) was prepared in dichloromethane (analytical grade, Shanghai Reagents). The concentration of BaP standard solution was diluted to 1.0 μg mL^{-1} by dichloromethane (DCM). The Stock 16 EPA polycyclic aromatic hydrocarbons (PAHs) mixture was purchased from Supelco (Bellefonte, PA, USA), including the following compounds: acenaphthene (1000 μg mL^{-1}), acenaphthylene (2000 μg mL^{-1}), anthracene (100.2 μg mL^{-1}), benzo(*a*)anthracene (99.9 μg mL^{-1}), benzo(*a*)pyrene (100.1 μg mL^{-1}), benzo(*b*)fluoranthene (200 μg mL^{-1}), benzo(*g*,*h*,*i*)perylene (199.9 μg mL^{-1}), benzo(*k*)fluoranthene (99.9 μg mL^{-1}), chrysene (100.2 μg mL^{-1}), dibenz(*a*,*h*)anthracene (199.9 μg mL^{-1}), fluoranthene (200 μg mL^{-1}), fluorene (200.1 μg mL^{-1}), indeno(1,2,3-CD)pyrene (100.1 μg mL^{-1}), naphthalene (1000 μg mL^{-1}), phenanthrene (100.1 μg mL^{-1}), and pyrene (99.9 μg mL^{-1}) (methanol–methylene chloride, 1 : 1). All of these solutions were prepared in volumetric flasks (with glass stoppers) wrapped with aluminium foil and stored in a refrigerator set at 4 °C.

3.3 Sample preparation

One gram of each vegetable oil sample was weighed into a filtering flask. Then 10 mL of 1 M methanolic potassium hydroxide solution was added to each sample followed by microwave-assisted saponification for 10 min. Meanwhile, a cup of 400 mL of water was placed in the microwave oven to avoid the sample overheating. After the samples were cooled down to ambient temperature, an aliquot of 15 mL ultrapure water was added into the flask and mixed well. The samples were extracted by 2 × 5 mL of dichloromethane (DCM) by ultrasonic extraction of 20 min each time. The organic extracts were carefully transferred and combined then diluted to 10 mL with DCM.

3.4 Spectral measurements

All synchronous fluorescence spectra were recorded at a scan speed of 240 nm min^{-1} and with excitation and emission bandpass both set to 5 nm. The constant-energy difference (wavenumber interval) between excitation and emission monochromators was 1400 cm^{-1}. Selection of this parameter was usually empirical.[18] Second-derivative spectra were then obtained by the electronic differentiator of the spectrofluorometer.

The standard addition method was applied to overcome possible matrix effects. Three concentration levels were added directly into the quartz cuvette, with a microlitre syringe, and analyzed. Two replicates were made for each calibration level. A small spiking volume (2 μL) being added to the extract solution was to minimize the change of the sample volume. The standard addition calibration curve was established by a regression of the peak-to-derivative baseline height of the second-derivative signal of BaP onto its added concentration. The concentration of the extract was obtained from extrapolation of the standard addition calibration curve.

4. Results and discussion

4.1 Second-derivative constant-energy synchronous fluorescence (DCESF) spectra of BaP

In the DCESF spectra of BaP standard solutions (Fig. 6(A)), the intensities of BaP main peaks (at 385 and 393.9 nm) increased linearly with the increase of BaP concentration. Due to the absence of matrix interference, the second-derivative curves intersected with one another at the zero baseline at points p_1 and p_2. The derivative-baseline coincided with the zero baseline. Fig. 6(B) shows the DCESF spectra of the coconut oil sample (certified reference material) added with the BaP standard concentration from 0 to 3.0 ng mL^{-1}, respectively. The curves intersected at two crossing points p_1 and p_2, and these two points clearly deviated from the zero baseline (dashed line). Therefore, we used the derivative baseline-correction method for overcoming the error caused by interference of unknown component (s) in the coconut oil. Quantification of BaP was performed by measuring the negative peak-to-derivative baseline height, which corresponded to the height between the derivative value at the negative peak and the value of the derivative baseline, indicated by h_1 in Fig. 6(B).

4.2 Validation of the method

The recoveries of the proposed method were determined by applying the full procedure to three replicates of each of peanut oil, corn oil, sunflower oil and olive oil to which BaP had been spiked with different concentrations. For each measurement, three samples were prepared and each spiked with the BaP standard solution at three different concentrations. The samples were thoroughly mixed for 30 min at room temperature. The recoveries of BaP obtained (three replicate analyses in each case) in this work ranged from 90.4 to 105.0%, and the mean recovery was 95.9 ± 4.3%. The relative standard error (RSD) was 1.1–4.2% (Table 3).

The accuracy of the proposed method was further evaluated by the application of the DCESFS method to the analysis of

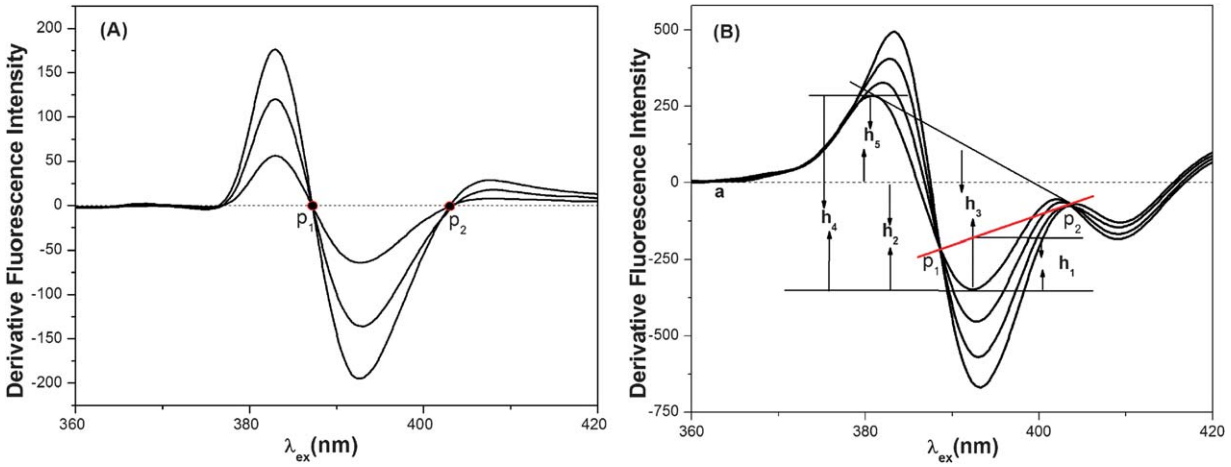

Fig. 6 (A) Second-derivative constant-energy synchronous fluorescence spectra of BaP standard solution (1.0∼3.0 ng mL^{-1}). (B) Second-derivative constant-energy synchronous fluorescence spectra of coconut oil (BCR-458) with the increase of added BaP standard solution (added concentration of BaP was 0∼3.0 ng mL^{-1}, respectively); dashed line is the zero baseline; red line is the derivative baseline. ($\Delta\bar{v} = 1400$ cm^{-1}, in DCM).

BaP in a certified reference material (coconut oil, BCR-458). The results obtained by different measurement methods for the BaP in coconut oil are shown in Table 4. Satisfactory results were obtained by the proposed method. The bias of the measured value from the certified value was −3.2%, which was much smaller than those obtained by other three methods.

4.3 Detection and quantification limits

An olive oil sample selected from vegetable oil samples which was found to have no detectable levels of BaP was used as a representative blank sample. As shown in Table 5, the limit of detection (LOD) and the limit of quantification (LOQ), calculated as 3SD/k and 10SD/k, respectively, were 0.16 and 0.53 μg kg^{-1}, where SD is the standard derivation of the 11 blank signals and k is the slope of the calibration equation. This was far below the acceptable threshold level of BaP (2.0 μg kg^{-1}) in oil, as restricted by the European Union.

4.4 Investigation of interference with the remaining 15 EPA PAHs

A number of other PAHs might also be present in vegetable oils. For the interference testing, we used a list of 16 priority PAHs, established by the Environmental Protection Agency (EPA), which have been most frequently detected in environmental samples. Fig. 7(A) shows the second-derivative constant-energy synchronous spectra of anthracene (An, red line, 2.0 ng mL^{-1}), benzo(k)fluoranthene (BkF, blue line, 2.0 ng mL^{-1}), BaP (solid black line, 2.0 ng mL^{-1}) standard solution, and the mixture of 16 PAHs (dashed black line, stock solution diluted to contain BaP 2.0 ng mL^{-1} by DCM). In the DCESF spectra of the 16 PAHs mixture, An and BkF exhibited fluorescence signals in DCM by using a constant-energy interval at 1400 cm^{-1}, which interfered the signals of BaP as the matrix interference when they were presented at concentration levels similar to BaP.

We used the proposed baseline-correction method to overcome this matrix interference. In Fig. 7(B), the derivative

Table 3 Recoveries of different added concentrations of BaP in vegetable oil samples

Samples	Measured/μg kg^{-1}	Added/μg kg^{-1}	Recovered mean/μg kg^{-1} ($n = 3$)	RSD (%)	Recovery (%)	Mean recovery ± SD (%)
Peanut oil	1.51	1.00	1.05	3.2	105.0	98.6 ± 5.5
		5.00	4.74	1.7	94.8	
		10.0	9.61	1.1	96.1	
Corn oil	2.00	1.00	1.03	3.7	102.7	97.4 ± 5.6
		5.00	4.58	2.2	91.6	
		10.0	9.78	2.2	97.8	
Sunflower oil	4.98	1.00	0.93	4.2	93.1	95.1 ± 1.9
		5.00	4.76	3.2	95.2	
		10.0	9.69	2.1	96.9	
Olive oil	1.34	1.00	0.91	4.2	91.0	92.5 ± 3.1
		5.00	4.52	2.2	90.4	
		10.0	9.60	1.7	96.0	

Table 4 Results of a certified reference material BCR-458 BaP in coconut oil by different measurement methods

Measurement method	Mean result/μg kg^{-1} (n = 3)	Certified value/μg kg^{-1}	Error (%)
Peak-to-derivative baseline (h_1 [a])	0.90 ± 0.08		−3.2
Negative peak-to-zero baseline (h_2 [a])	0.58 ± 0.09		−37.7
Tangent method (h_3 [a])	1.08 ± 0.12	0.93 ± 0.09	+16
Peak-to-trough (h_4 [a])	0.98 ± 0.07		+5.4
Positive peak-to-zero baseline (h_5 [a])	1.15 ± 0.09		+24

[a] h_1, h_2, h_3, h_4 and h_5 were marked as in Fig. 6(B).

Table 5 Linear relationships and limits of detection and quantification of BaP

Linear range/μg kg^{-1}	Calibration equation[a]	Correlation coefficient (r)	Blank signal (mean ± SD)[b]	LOD/μg kg^{-1}	LOQ/μg kg^{-1}
0–50.0	$I = 109.1C + 1.3$	0.9995	1.3 ± 0.58	0.16	0.53

[a] I: fluorescence intensity; C: concentration/ng mL^{-1}. [b] SD: Standard error.

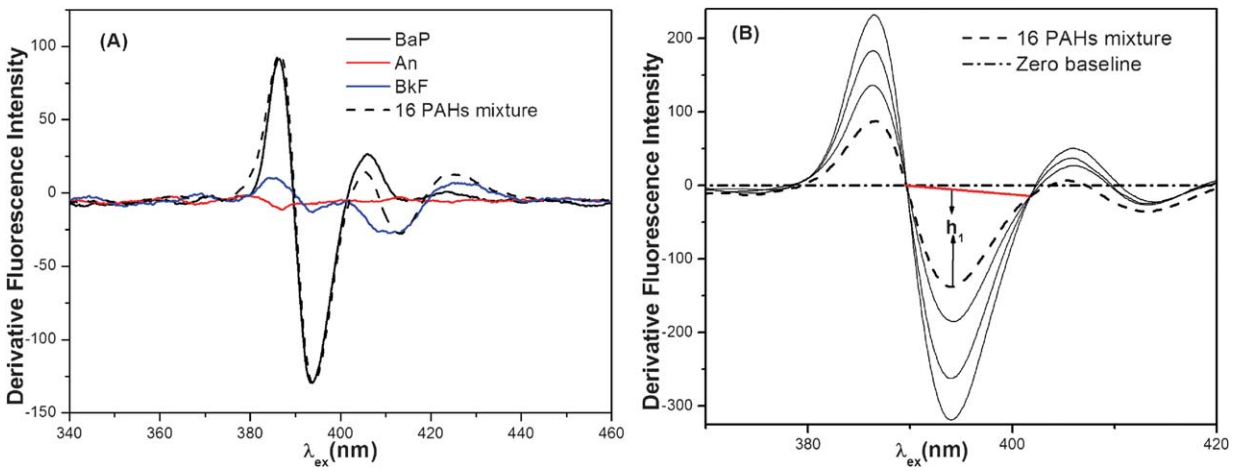

Fig. 7 (A) The DCESF spectra of An (red curve, 2.0 ng mL^{-1}), BkF (blue curve, 2.0 ng mL^{-1}), BaP (solid black curve, 2.0 ng mL^{-1}) standard solution, and 16 PAHs mixture (dashed black curve, the stock solution was diluted to BaP 2.0 ng mL^{-1} by DCM). (B) 16 PAHs mixture (containing BaP 2.0 ng mL^{-1}) with increasing amounts of added BaP standard concentration from 0 to 3.0 ng mL^{-1}, respectively; the red line is the derivative baseline, $\Delta\bar{v} = 1400$ cm^{-1}.

baseline (red line) deviated from the zero-baseline in the range of the negative peak of BaP owing to the interference of An and BkF. Satisfactory results were obtained by the proposed method for BaP in mixtures of 16 EPA PAHs and the relative error of the measured value (1.95 ± 0.08 ng mL^{-1}, n = 3) from the certified value (2.0 ng mL^{-1}) was +2.6%. Therefore, the proposed baseline-correction method can be used for accurate analysis of BaP in the presence of the remaining 15 EPA PAHs.

5. Conclusions

In the present study, a novel baseline-correction method for derivative spectra based on SAM was firstly proposed for the reduction of errors caused by band overlaps in quantitative analysis, especially when the interfering spectrum was a broad unknown band, which is common in practical analysis. By simply analyzing the derivative spectra of standard solutions of analyte added, the accurate results could be easily obtained free of tedious separation. Thus, the combination of SAM and the derivative technique can be used to eliminate not only the matrix effect, but also the matrix interference of unknown components with the application of the proposed baseline-correction method. The shape of the baseline is a crucial factor influencing the quantification. In this study we have discussed in detail the parameters of the interfering band affecting the derivative baseline. The proposed method is especially suitable when the derivative curve of interference between two crossing points is close to a straight line. The proposed baseline-correction method is more efficient in background removal than other commonly-used measurement methods (the peak-to-zero baseline method,

the tangential approximation method, and the peak-to-trough method). Potentially the proposed method can be applied to various types of derivative spectra in different fields such as UV-visible spectroscopy, fluorescence spectroscopy and infrared spectroscopy. Both the simulation analysis and the experimental results suggest satisfactory performance of the proposed method. The proposed method provided a promising, simple and cost-effective tool for routine analytical work.

Acknowledgements

Financial support from National Natural Science Foundation of China (20975084), Science and Technology program of Fujian Province (2009Y0046) and the 973 program of China (2007CB935600) are highly acknowledged. We thank Dr Yu-Luan Chen and Dr Chun Wu for critical reading of this manuscript.

References

1 V. J. Hammond and W. C. Price, *J. Opt. Soc. Am.*, 1953, **43**, 924–929.
2 A. T. Giese and C. S. French, *Appl. Spectrosc.*, 1955, **9**, 78–96.
3 A. E. Martin, *Nature*, 1957, **180**, 231–233.
4 J. P. Pemsler, *Rev. Sci. Instrum.*, 1957, **28**, 274–275.
5 F. Sánchez Rojas, C. Bosch Ojeda and J. M. Cano Pavón, *Talanta*, 1988, **35**, 753–761.
6 C. Bosch Ojeda, F. Sanchez Rojas and J. M. Cano Pavon, *Talanta*, 1995, **42**, 1195–1214.
7 C. Bosch Ojeda and F. Sánchez Rojas, *Anal. Chim. Acta*, 2004, **518**, 1–24.
8 F. Sánchez Rojas and C. Bosch Ojeda, *Anal. Chim. Acta*, 2009, **635**, 22–44.
9 H. Susi and D. M. Byler, *Biochem. Biophys. Res. Commun.*, 1983, **115**, 391–397.
10 C. E. Cooper, C. E. Elwell, J. H. Meek, S. J. Matcher, J. S. Wyatt, M. Cope and D. T. Delpy, *Pediatr. Res.*, 1996, **39**, 32–38.
11 A. P. Fernández-Getino, Z. Hernández, A. Piedra Buena and G. Almendros, *Geoderma*, 2010, **158**, 225–232.
12 A. A. Christy, *Vib. Spectrosc.*, 2010, **54**, 42–49.
13 W. K. Fowler, D. O. Knapp and J. D. Winefordner, *Anal. Chem.*, 1974, **46**, 601–602.
14 J. L. Magnin, L. A. Decosterd and C. Centeno, *Pharm. Acta Helv.*, 1996, **71**, 237–246.
15 H. W. Sun, Y. Gao, C. G. Yuan, Y. X. Zhang, L. L. Yang and D. Q. Zhang, *Anal. Sci.*, 2002, **18**, 325–328.
16 G. L. Green and T. C. O'Haver, *Anal. Chem.*, 1974, **46**, 2191–2196.
17 P. John and I. Soutar, *Anal. Chem.*, 1976, **48**, 520–524.
18 A. Andrade-Eiroa, G. de-Armas, J. M. Estela and V. Cerdà, *TrAC, Trends Anal. Chem.*, 2010, **29**, 902–927.
19 Y. Q. Li, X. Z. Huang, J. G. Xu and G. Z. Chen, *Anal. Chim. Acta*, 1992, **256**, 285–291.
20 M. I. Walash, F. Belal, N. El-Enany and A. Abdelal, *J. Fluoresc.*, 2008, **18**, 61–74.
21 K. Mohammadpour, M. R. Sohrabi and A. Jourabchi, *Talanta*, 2010, **81**, 1821–1825.
22 Q. J. Gong, J. L. Qiao, L. M. Du, C. Dong and W. J. Jin, *Talanta*, 2000, **53**, 359–365.
23 M. C. Mahedero García, N. Mora Diez, D. Bohoyo Gil and F. S. López, *J. Pharm. Biomed. Anal.*, 2005, **38**, 349–354.
24 M. M. Karim, C. W. Jeon, H. S. Lee, S. M. Alam, S. H. Lee, J. H. Choi, S. O. Jin and A. K. Das, *J. Fluoresc.*, 2006, **16**, 713–721.
25 N. A. Charoo and M. Bashir, *Anal. Lett.*, 2009, **42**, 2232–2243.
26 O. A. Donmez, Bozdogan, A. G. Kunt and Y. Div, *J. Anal. Chem.*, 2010, **65**, 30–35.
27 A. Andrade Eiroa, E. Vázquez Blanco, P. López Mahía, D. Prada Rodríguez and E. Fernández Fernández, *Analyst*, 2000, **125**, 1321–1326.
28 T. Galeano Díaz, I. Durán Merás and D. Airado Rodríguez, *Anal. Bioanal. Chem.*, 2007, **387**, 1999–2007.
29 J. T. Grant, *J. Surf. Anal.*, 2008, **15**, 123–129.
30 D. Kul, *J. AOAC Int.*, 2010, **93**, 882–890.
31 J. S. Millership and J. Chin, *J. Anal. Chem.*, 2010, **65**, 164–168.
32 A. A. M. Wahbi, M. A. Abounassifa and H. M. G. Alkahtani, *J. Pharm. Biomed. Anal.*, 1989, **7**, 39–43.
33 S. Altinöz and D. Tekeli, *J. Pharm. Biomed. Anal.*, 2001, **24**, 507–515.
34 D. A. Barkauskas and D. M. Rocke, *Anal. Chim. Acta*, 2010, **657**, 191–197.
35 D. Chen, F. Wang, X. G. Shao and Q. D. Su, *Analyst*, 2003, **128**, 1200–1203.
36 X. G. Shao, C. Y. Pang and Q. D. Su, *Fresenius J. Anal. Chem.*, 2000, **367**, 525–529.
37 X. G. Shao and C. X. Ma, *Chemom. Intell. Lab. Syst.*, 2003, **69**, 157–165.
38 Z. M. Zhang, S. Chen and Y. Z. Liang, *Analyst*, 2010, **135**, 1138–1146.
39 L. Maurice-Estepa, P. Levillain, B. Lacour and M. Daudon, *Clin. Chim. Acta*, 2000, **298**, 1–11.
40 M. Benamor and N. Aguerssif, *Spectrochim. Acta, Part A*, 2008, **69**, 676–681.
41 A. H. Patel, J. K. Patel, K. N. Patel, G. C. Rajput and N. B. Rajgor, *J. Pharm. Biomed. Anal.*, 2010, **1**, 1–5.
42 M. D. G. García, M. J. Culzoni, M. M. D. Zan, R. S. Valverde, M. M. Galera and H. C. Goicoechea, *J. Chromatogr., A*, 2008, **1179**, 115–124.
43 Bo E. H. Saxberg and B. R. Kowalski, *Anal. Chem.*, 1979, **51**, 1031–1038.
44 J. H. Kalivas and B. R. Kowalski, *Anal. Chem.*, 1981, **53**, 2207–2212.
45 J. H. Kalivas, *Anal. Chem.*, 1983, **55**, 565–567.
46 W. R. Kelly, B. S. MacDonald and W. F. Guthrie, *Anal. Chem.*, 2008, **80**, 6154–6158.
47 T. C. O'Haver and G. L. Green, *Anal. Chem.*, 1976, **48**, 312–318.
48 D. L. Lin, L. F. He and Y. Q. Li, *Clin. Chem.*, 2004, **50**, 1797–1803.
49 F. He, D. L. Lin and Y. Q. Li, *Anal. Sci.*, 2005, **21**, 641–645.
50 N. Zhou, H. D. Luo, N. Li, Y. Z. Jia and Y. Q. Li, *Luminescence*, 2011, **26**, 35–43.

